Applied Radiation and Isotopes 112 (2016) 31–37

Contents lists available at ScienceDirect

Applied Radiation and Isotopes

journal homepage: www.elsevier.com/locate/apradiso

A plastic scintillator-based 2D thermal neutron mapping system for use in BNCT studies

N. Ghal-Eh [a,*], S. Green [b,c]

[a] School of Physics, Damghan University, 36716-41167, Damghan, Iran
[b] School of Physics and Astronomy, University of Birmingham, Birmingham B15 2TT, United Kingdom
[c] Hall Edwards Radiotherapy Research Group, Department of Medical Physics, University Hospital Birmingham, Birmingham B15 2TH, United Kingdom

HIGHLIGHTS

- A plastic scintillator-based instrument is proposed for thermal neutron mapping in water phantom.
- A two-dimensional map of thermal neutrons is presented based on 2.22 MeV gamma-ray detection.
- The whole system has been simulated using Monte Carlo code MCNPX 2.6.
- The results confirm that the thermal flux peaks between 2 cm and 4 cm distance from the system entrance.

ARTICLE INFO

Article history:
Received 9 December 2015
Received in revised form
2 March 2016
Accepted 2 March 2016
Available online 4 March 2016

Keywords:
BNCT
MCNP
Scintillator
Thermal neutrons

ABSTRACT

In this study, a scintillator-based measurement instrument is proposed which is capable of measuring a two-dimensional map of thermal neutrons within a phantom based on the detection of 2.22 MeV gamma rays generated via $n_{th}+H\rightarrow D+\gamma$ reaction. The proposed instrument locates around a small rectangular water phantom (14 cm × 15 cm × 20 cm) used in Birmingham BNCT facility. The whole system has been simulated using MCNPX 2.6. The results confirm that the thermal flux peaks somewhere between 2 cm and 4 cm distance from the system entrance which is in agreement with previous studies.

1. Introduction

Boron neutron capture therapy (BNCT) is a binary form of radiotherapy based on the administration of a ^{10}B-compound which accumulates in the tumour at higher concentration than in healthy tissues, and on the successive irradiation of the target with low energy neutrons (Hatanaka, 1987). Thermal neutron capture in ^{10}B, with a cross section of 3837 b at thermal energies, gives rise to high-LET radiation, generating an alpha particle and a ^{7}Li nucleus with ranges in tissues comparable to a cell diameter. As the energy deposition is spatially confined in the cells where neutrons are captured, dose delivery is selective at a cellular level without requiring the irradiation field to tightly match the shape of the target. This characteristic makes BNCT a potential option for the tumours that cannot be surgically removed nor treated with a conventional radiotherapy (Farías et al., 2014).

It is necessary to have a high flux of thermal neutrons in the region of the tumours to be treated. For tumours which are deep in the body, it becomes necessary to target the patient with a flux of higher energy neutrons (i.e., epithermal). These in turn become moderated as they pass through overlying tissue, ultimately delivering the required thermal neutron fluence to which boron reacts so favorably. This means that a high flux of thermal neutrons at the tumour position makes the radiotherapy treatment selective and confirms that determination of the thermal neutron flux distribution is one of the most important quality assurance (QA) steps in BNCT treatment.

A variety of detection techniques have been proposed for BNCT QA which can be categorized in three groups: (1) techniques relying on the prompt-gamma (i.e., ^{7}Li*478 keV de-excitation gamma rays) such as those called BNCT-SPECT (McGregor et al., 1996), (2) epithermal neutron measurement techniques (such as those incorporating resonance absorption filters) (Ghal-Eh et al., 2007) and (3) thermal neutron measurements which are mostly passive and based on neutron activation (Mostafaei et al., 2015).

The present study aims to present a reliable tool for thermal

* Corresponding author.
E-mail address: ghal-eh@du.ac.ir (N. Ghal-Eh).

http://dx.doi.org/10.1016/j.apradiso.2016.03.002
0969-8043/

neutron measurement (within the framework of group (3) of the above mentioned categories). Section 2 reviews the thermal neutron measurement methods that are currently implemented in BNCT studies with the emphasis on the need for an on-line thermal neutron measurement system.

The idea for the proposed system is a special position-sensitive array detector mostly used in astrophysics applications. In the present application a 2D map of the thermal neutrons within the phantom is measured which will be discussed in Section 3. Section 4 presents the details of the proposed system together with the MCNP simulation results for an incident epithermal neutron beam.

2. Research background

2.1. Thermal neutron measurement methods

A detailed knowledge of the thermal flux distribution in a phantom is important for understanding the boron dose in BNCT. Thermal neutron flux simulations with Monte Carlo codes depend on accurate cross sections and also need experimental verification.

Thermal neutron measurement is basically undertaken either through neutron-induced nuclear reactions with suitable nuclei (i.e., with high thermal neutron absorption cross section) such as ^{6}Li, ^{10}B and ^{3}He or through neutron capture reactions with nuclei such as indium, copper, gold or thermoluminescence compounds. Utilising these reactions, the neutron flux at a BNCT facility is measured by a variety of methods, the most common being foil activation cadmium difference instruments, ionization chambers with deposited fission converter material or TLDs. The cadmium difference method requires two separate irradiations at a beam port and post irradiation measurements of the induced gamma activity. Cadmium cut-off energy can also be used as neutron energy separator in a Monte Carlo simulation package for thermal neutron flux calculation. The energy dependence of cadmium neutron capture cross section differs from the ^{10}B cross section. TLD is not a direct method of thermal neutron flux measurement but requires an independent calibration. Unshielded fission counters, ^{3}He-filled and BF_3 ion chambers are also used at reactor-based BNCT to monitor the residual thermal neutron flux.

Almost all commonly-used techniques described above do not really map the thermal flux in an on-line manner. In the present study, the approach which has been mainly used by astrophysicists, is developed for a 2D thermal neutron mapping inside a small water phantom.

2.2. Orthogonal position-sensitive measurement system

In 1977, Gerber et al. introduced a position-sensitive gamma-ray detector in which two orthogonal arrays of semi-conductor detectors were proposed, with the idea of using a coincidence circuit between detector banks (Gerber et al., 1977) (Fig. 1.). Similar efforts but in different applications have been made by Amman and Luke (2001) using germanium detectors, Bravar et al. (2006) for fast neutron detection with plastic scintillators, Nelson (2012) for a system similar to SPECT, Cruceru et al. (2013) for heavy charged particle detections and by Binns et al. (2014) for the detection of ultra-heavy galactic cosmic rays.

The orthogonal position-sensitive systems operate based on the coincident signals from two perpendicular detectors that are hit by crossing incident particle that can deposit enough energy in both detectors. This system can be modified as shown in Fig. 2.

As seen, neglecting the coincidence circuitry for the moment, the two detector arrays have been separated to allow a specific rectangular object (i.e., the water phantom) to be placed in between. The purpose is to locate the xz position of the radiation source within the rectangular object with pulse-height information taken from the two detector sets. The geometry details and the Monte Carlo simulations of the proposed system with the MCNPX code (McKinney et al., 2007) are provided in Section 3.

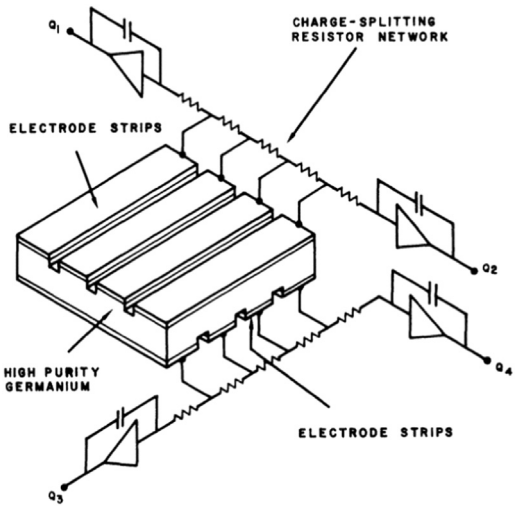

Fig. 1. The orthogonal-strip position-sensitive detector proposed by Gerber et al. (1977).

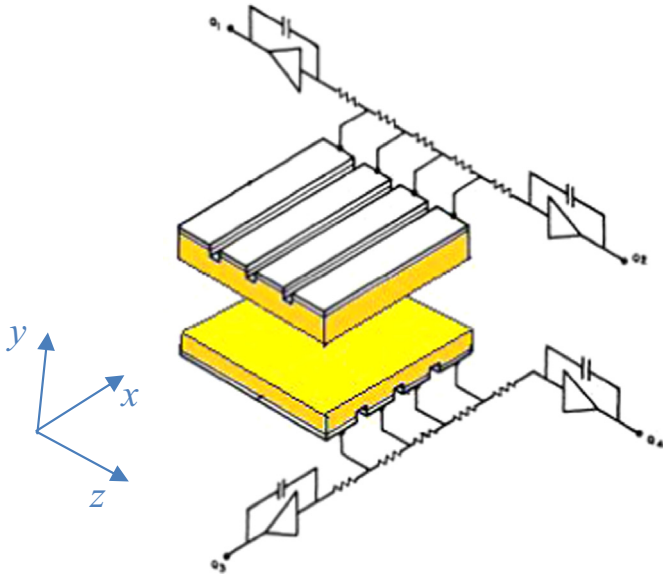

Fig. 2. Modified orthogonal-strip position-sensitive detector.

3. 2D thermal mapping system

The basis of the Birmingham BNCT project is the 3 MV Dynamitron accelerator situated at the University of Birmingham in which a beam of relatively low-energy (~2.8 MeV) protons are bombarded onto a thick natural lithium target and neutrons are produced according to the ^{7}Li(p,n)^{7}Be reaction. The accelerator has demonstrated proton currents in excess of 1 mA producing a neutron intensity of 1.37×10^{12} n/s. In order to reach the epithermal energies required for therapy in BNCT a special beam-shaping assembly (BSA) made of Fluental™ (69% AlF_3/30% Al/1% LiF) as moderator, graphite as reflector and lithiated polyethylene as absorber has been constructed. The schematics of the BSA and the small ($14 \times 15 \times 20$ cm^3) rectangular water phantom are shown in

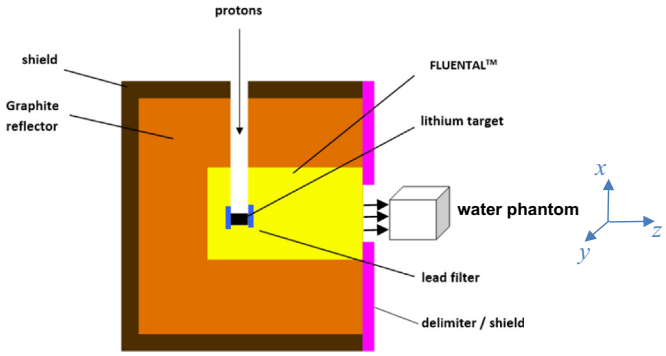

Fig. 3. Schematic diagram of the neutron moderating system and rectangular water phantom.

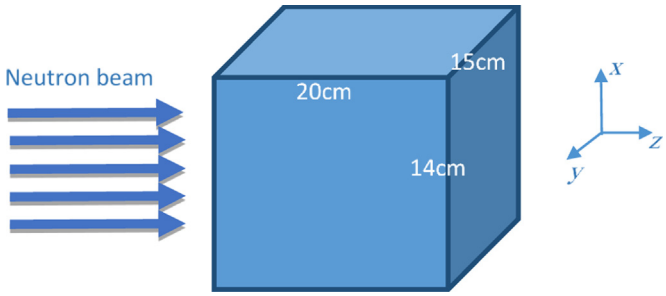

Fig. 4. The rectangular water phantom. The neutrons are incident on the xy surface in +z direction.

Figs. 3 and 4, respectively.

The proposed thermal neutron mapping system has been designed to be placed around the water phantom. The system consists of seventeen rectangular NE102 plastic scintillators (seven $2\times2\times20$ cm^3 and ten $2\times2\times14$ cm^3). All seventeen scintillators are intended to be coupled onto 2×2 cm^2 square-window photomultiplier tubes (PMTs) as shown in Fig. 5.

The xz projection of the two orthogonal scintillator sets forms a mesh of 70 pixels of 2×2 cm^2 area. Similar mesh tiles may be considered on the xz surface of the water phantom (i.e., 70 equal-volume water voxels of $2\times2\times15$ cm^3). The opposing banks of detectors are not operated in a coincidence mode in this application.

MCNPX simulations have been performed to evaluate the thermal neutron flux within the water phantom when a broad beam of 1 keV neutrons are incident on the xy plane of the water phantom. As seen in Fig. 6, the thermal flux (i.e., with energies below 1 eV) peaks at the second horizontal pixels (i.e., somewhere between 2 cm and 4 cm away from the beam entrance) which is in agreement with previous experimental (Binns et al., 2005) and Monte Carlo (Rassow et al., 2001) studies. It is most desirable if the proposed system can provide similar results within the limits of its 2-cm spatial resolution.

It is well known that H(n,γ(2.22 MeV))D reaction occurs as soon as neutrons are thermalized inside water. The positions at which 2.22 MeV gamma rays are emitted are regarded as thermal neutron interaction points. Hence the thermal neutron distribution mapping may be obtained by locating (i.e., imaging) the 2.22 MeV gamma rays.

Several geometries have been examined to obtain an optimum configuration for the system. The collimator geometry and the thickness of necessary thermal neutron shielding have been determined with MCNP simulations. Two relatively thick (10 cm) lead collimators have been chosen at both sides between the water phantom and plastic scintillator arrays. Such a thick collimator can suppress approximately 99.4% of the 2.22 MeV gamma rays and for

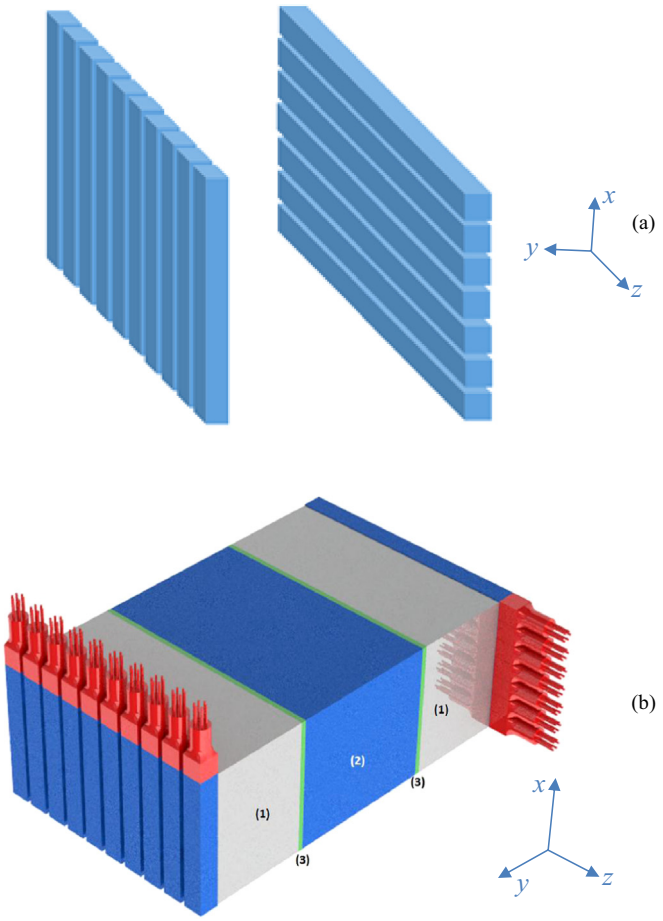

Fig. 5. (a) Two sets of orthogonal plastic scintillators to be placed around the water phantom. (b) The detection system consists of horizontal and vertical scintillators, thick lead collimator blocks (1), rectangular water phantom (2), thin cadmium sheets (3) and 17 PMTs.

which the suitable thickness can be simply calculated using the gamma ray linear attenuation coefficient (NIST). Each collimator block has 280 cylindrical holes of 3 mm radii. To avoid thermal neutron interaction with both plastic scintillators and PMT windows and to enhance signal-to-noise ratio, a 5 mm cadmium layer has been placed between the water phantom and lead collimator. The top view of the proposed system and the neutron flux are illustrated in Fig. 7. The neutron-induced gamma-rays are propagated inside the water phantom and eventually deposit energies within the plastic scintillator arrays after travelling through the narrow collimators. The gamma-ray deposition energy plot is shown in Fig. 8 whilst Fig. 9 shows the pulse-height distributions of both horizontal and vertical plastic scintillators. As shown in Fig. 9, unlike inorganics, the plastic scintillators do not represent full-energy peak (i.e., photopeak) due to their relatively low photo-electric interaction cross section which is mainly because of low-Z constituents and density.

Having calculated the required pulse-height spectra from both horizontal and vertical scintillators, the thermal neutron distribution imaging strategy was the next important step. Since our preliminary measurement studies focus on a 2D image, the general reconstruction procedures normally used for 3D imaging are not necessary. Several mathematical models have been checked but finally it has been decided to simply use the multiplication of horizontal scintillator counts by vertical ones to obtain 70 different values corresponding to 70 square pixels. Here the scintillator counts refer to the area under the spectrum from 2.0 to 2.3 MeV as a measure of those gamma rays received by the scintillators without serious energy loss when travelling through long air holes

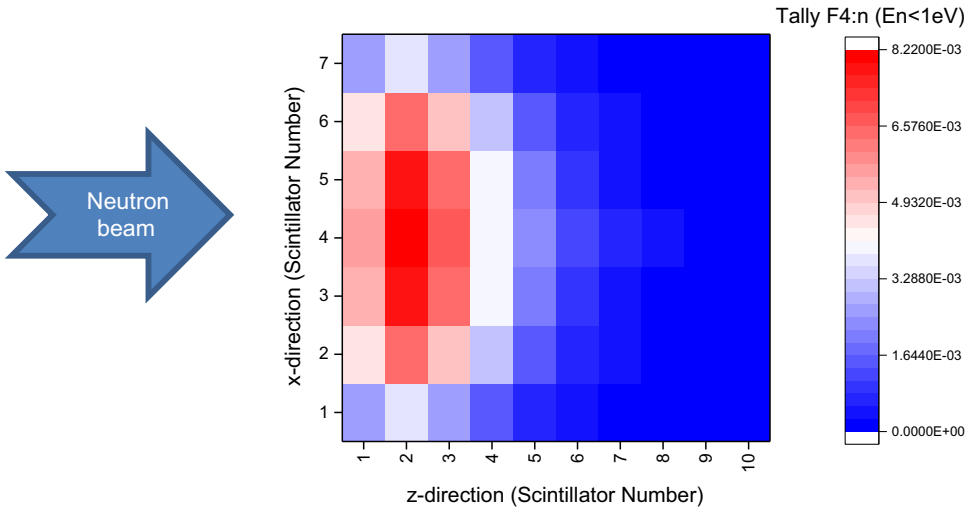

Fig. 6. The thermal (i.e., En < 1 eV) neutron flux distribution within a rectangular phantom.

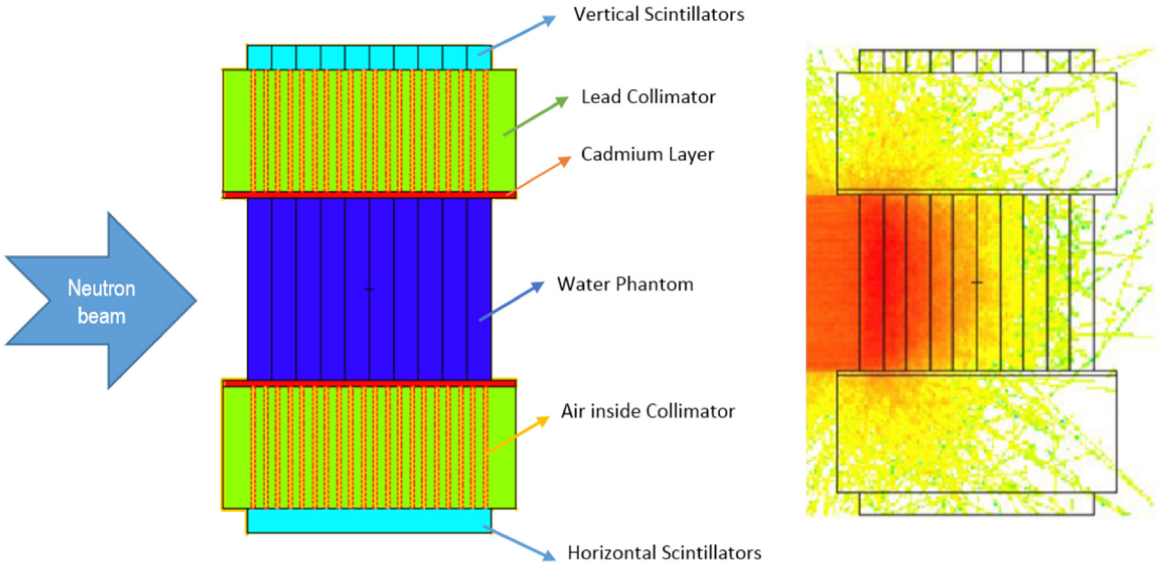

Fig. 7. (Left) The MCNP-generated plot of the proposed thermal neutron imaging system (top view). (Right) The MCNPX mesh tally plot of neutron flux.

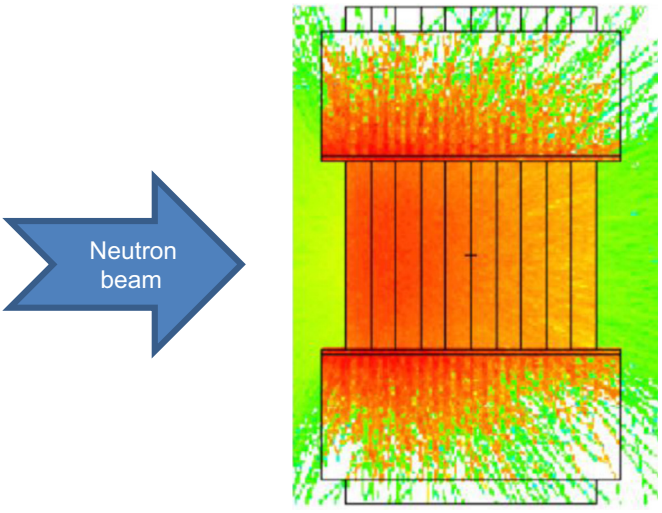

Fig. 8. Neutron-induced gamma ray deposition energy mesh tally plot when the measurement system is exposed to a broad beam of 1 keV neutrons.

inside thick lead collimators. This so-called pulse-height threshold can be undertaken by setting appropriate lower-level discriminator in practical application.

Also the ambient or background gamma rays have been neglected in the present setup. However, for practical purposes, an appropriate gamma ray shield is necessary for obtaining an unblurred image.

In order to check the image-reconstruction procedure for the proposed measurement system, a point source of 2.22 MeV gamma rays has been considered at different positions inside the water phantom. As seen in Fig. 10, the reconstructed images well agree with the input data. A numerical example for the image reconstruction has been given in Section 4.

4. Results and discussion

The thermal neutron profile within the water phantom is the most important information required for quality assurance of a BNCT beam. In this paper, a proposed system has been designed to be placed around the small water phantom, consisting seven 2 ×

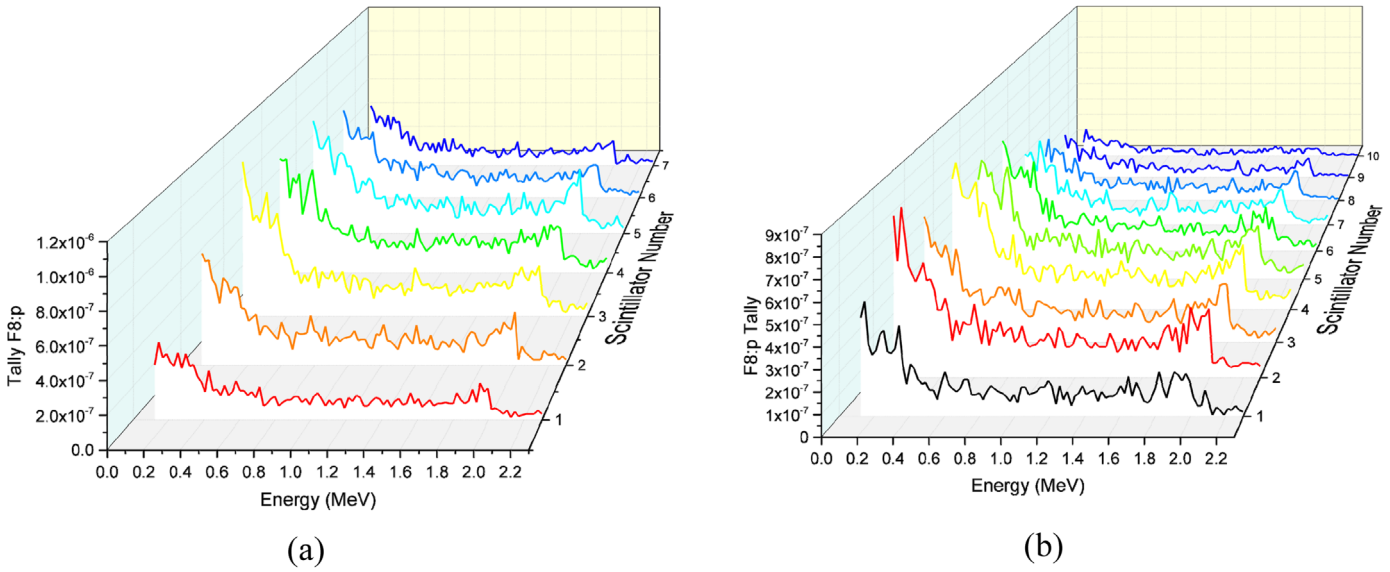

Fig. 9. The pulse-height distribution of (a) horizontal and (b) vertical NE102 scintillators when the water phantom is irradiated with a broad beam of 1 keV neutrons.

2×20 cm^3 and ten $2 \times 2 \times 14$ cm^3 NE102 scintillators coupled onto 2×2 cm^2 square-window PMTs. The typical tally F8 values for both horizontal and vertical scintillators when exposed to a beam of 1 keV neutrons together with image matrix values produced through multiplications have been presented in Table 1. The corresponding constructed image is also shown in Fig. 11.

As seen in Figs. 12 and 13, although both the thermal flux and the reconstructed image show that the thermal flux peak occurs at the second vertical scintillator, the image exhibits a thermal neutron spread towards the end of the water phantom. The difference may be attributed to the penetration of radiation (gamma rays or secondary electrons) from one scintillator to the neighboring ones (i.e. cross-talk), which apparently disturbs the imaging resolution. The existence of cross-talk has been examined by considering unrealistic dense scintillators in MCNP simulation and also by setting a specific scintillator as void. In the physical system (which has not yet been constructed) it is anticipated that this problem may be resolved by setting up two separate anti-coincidence circuits, one among seven horizontal scintillators and the other between ten vertical ones. This is purely to suppress cross-talk between adjacent scintillators. There is no coincidence requirement between the opposing banks of scintillators (as there would be in a PET detection system). Since the anti-coincidence circuit does not generate output if its input signals are produced within a short time interval, any penetration from one scintillator to another (normally between two adjacent scintillators) is vetoed.

The presented image shows a clear sensitivity to the incident neuron energy. As seen in Fig. 14, the thermal neutron concentration moves forward as neutron energy increases. From our calculations, the proposed system would be able to easily discriminate a change from an incident neutron energy of 0.5–1 keV (data not shown) and from 1 keV to 10 keV (as shown in Fig. 14). Further work is required to quantify the minimal detectable change in incident beam energy across a wider energy range.

In this paper an incident epithermal beam has been considered, however in principle such a system could also be applied to an incident thermal neutron beam or indeed to a “mixed” beam as sometimes used clinically for BNCT. In this proof-of concept study, a 2-cm spatial resolution has been used and only 2D reconstruction adopted of the thermal fluence within a small rectangular phantom of approximately the size of a human head. All of these choices could be reviewed for a final clinical system. Neutron beams used for BNCT tend to have simple circular or rectangular cross sections so 2D reconstruction is likely to be sufficient.

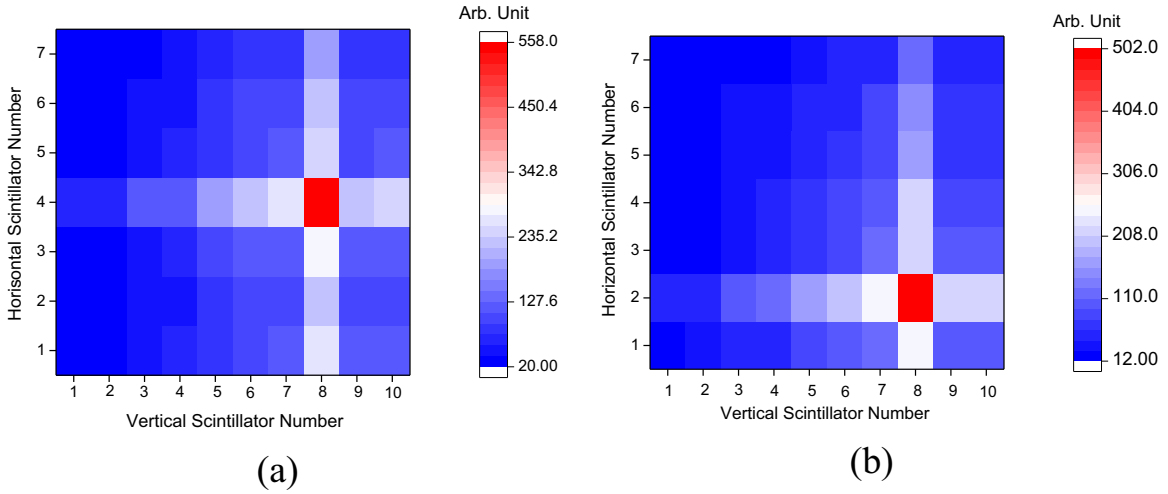

Fig. 10. The reconstructed image when the point 2.22 MeV gamma-ray source is located at (a) (x,y,z)=(0 cm, 0 cm, 5 cm) and (b) (x,y,z)=(−4 cm, 0 cm, 5 cm).

Table 1
The tally F8 values (in arbitrary unit) calculated for horizontal and vertical scintillators when exposed to a broad beam of 1 keV neutrons. The image matrix elements which are further converted into pixel intensities have been calculated through simple multiplication of vertical by horizontal scintillators' values.

		Vertical Scintillators: Typical F8 Values									
		17.29	21.62	20.80	17.53	14.59	10.59	7.13	4.86	3.61	2.02
Horizontal Scintillators: Typical F8 Values	1.12	19.36	24.21	23.30	19.63	16.34	11.86	7.99	5.44	4.04	2.26
	1.74	30.08	37.62	36.19	30.50	25.39	18.43	12.41	8.46	6.28	3.51
	2.04	35.27	44.10	42.43	35.76	29.76	21.60	14.55	9.91	7.36	4.12
	2.27	39.25	49.08	47.22	39.79	33.12	24.04	16.19	11.03	7.97	4.59
	2.03	35.10	43.89	42.22	35.59	29.62	21.50	14.47	9.87	7.33	4.10
	1.69	29.22	36.54	35.15	29.63	24.66	17.90	12.05	8.21	6.10	3.41
	1.06	18.33	22.92	22.05	18.58	15.47	11.23	7.56	5.15	3.83	2.14
		Evaluated Values									

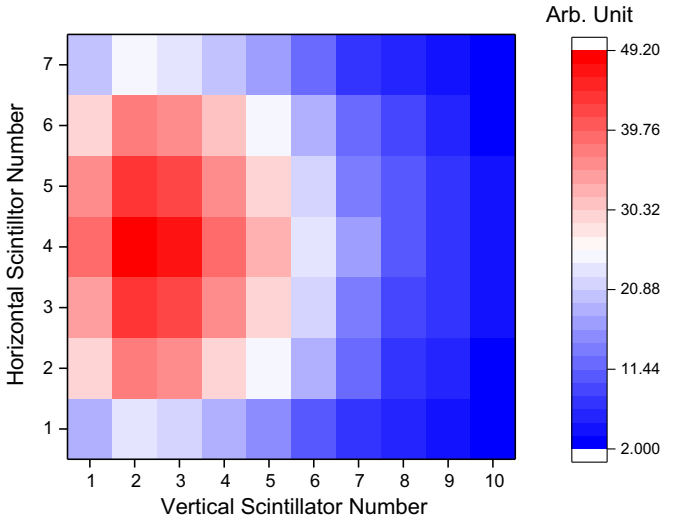

Fig. 11. The 2D thermal neutron image reconstructed through the multiplication of vertical by horizontal scintillators F8 values taken from Table 1.

Nevertheless the approach described here is generalizable to 3D reconstruction and indeed could be applied to any phantom geometry. In terms of spatial resolution, for clinical use it is likely that in the first 3–4 cm from the phantom surface a higher spatial resolution would deliver some advantages, and perhaps 0.5 cm would be closer to the optimum resolution. This would be helpful for both thermal and epithermal beam incidence. Beyond around 4 cm deep, the relatively slow and smooth variation of thermal fluence with depth means that 2 cm spatial resolution is likely to be sufficient.

5. Concluding remarks

The development of a reliable and real-time instrument for thermal neutron flux mapping inside a water phantom is an important issue in clinical applications of BNCT within the framework of pre-treatment QA. In this research, a measurement system consists of 17 commercially-available plastic scintillators and PMTs together with some shielding/collimator materials of special geometry, has been proposed.

The Monte Carlo simulations with MCNPX code show that the proposed system can generate 2D image of thermal neutron flux distribution with 2-cm spatial resolution based on the detection of 2.22 MeV gamma rays. The system also exhibits an acceptable sensitivity to incident neutron energy. The image quality enhancement can be performed by incorporating appropriate anti-coincidence circuits, one among seven horizontal scintillators and the other between ten vertical ones which is still being investigated.

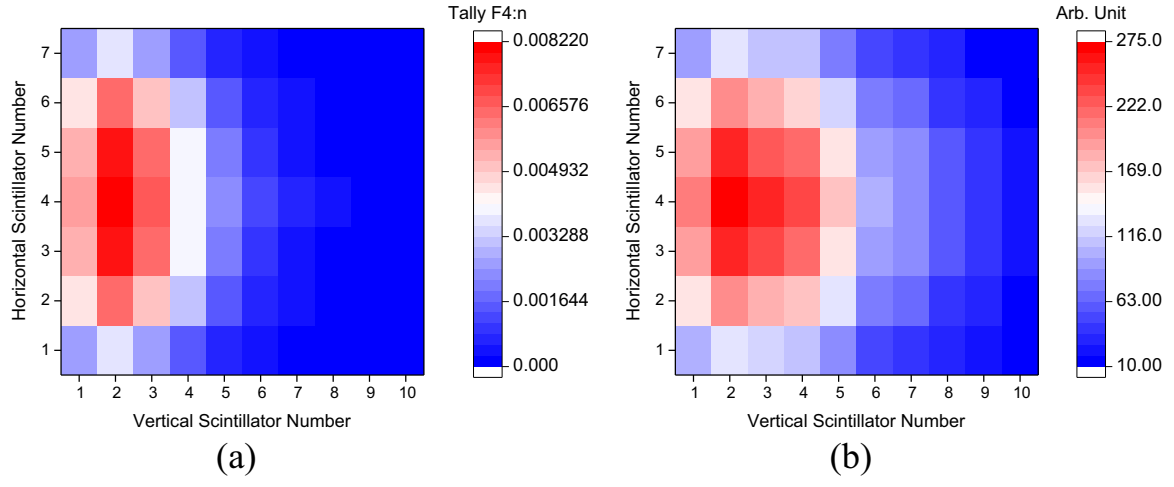

Fig. 12. A 2D plot of (a) MCNP-simulated thermal neutron flux within a small water phantom and (b) a reconstructed image obtained from the pulse-heights of horizontal and vertical scintillators.

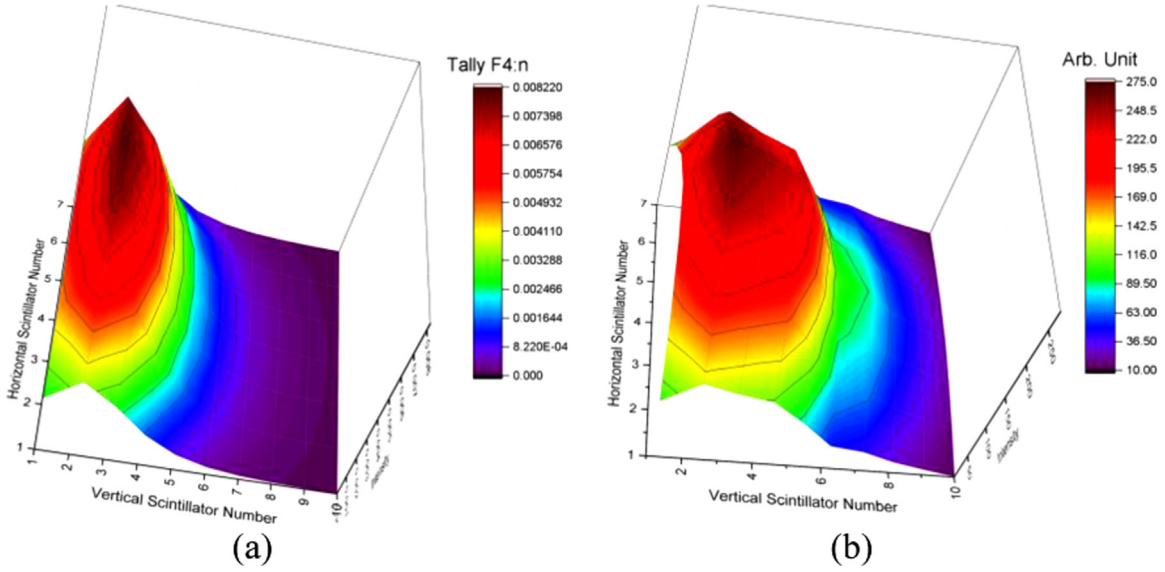

Fig. 13. A 3D plot of (a) MCNP-simulated thermal neutron flux within a small water phantom and (b) a reconstructed image obtained from the pulse-heights of horizontal and vertical scintillators.

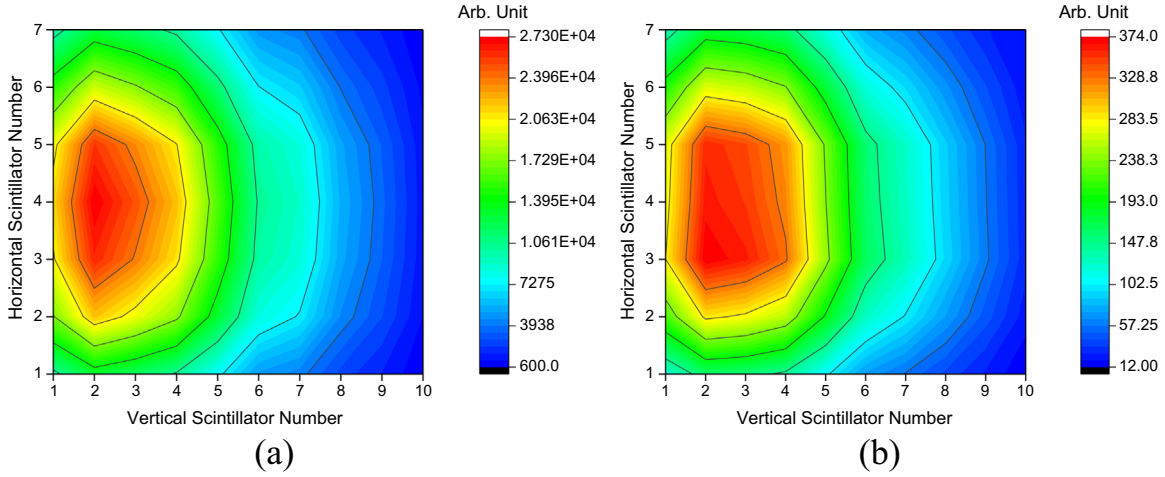

Fig. 14. A 2D contour plot version of thermal neutron reconstructed image for an incident rectangular beam of different energies: (a) 1 keV and (b) 10 keV.

Acknowledgements

We are grateful to anonymous reviewers for careful reading of the manuscript and their helpful comments. Also, the first author (NG) would like to thank both the School of Physics and Astronomy, University of Birmingham, U. K., for the research support and Damghan University, Iran, (PHYS1393) for the short-visit grant.

References

Amman, M., Luke, P., 2001. Three-Dimensional Position-Sensitive Germanium Detectors (No. EMSP-65015). Lawrence Berkeley National Lab., Berkeley, CA (US).

Binns, P.J., Riley, K.J., Harling, O.K., 2005. Epithermal neutron beams for clinical studies of boron neutron capture therapy: a dosimetric comparison of seven beams. Radiat. Res. 164 (2), 212–220.

Binns, W.R., Bose, R.G., Braun, D.L., Brandt, T.J., Daniels, W.M., Dowkontt, P.F., Fitzsimmons, S.P., Hahne, D.J., Hams, T., Israel, M.H., Klemic, J., 2014. The SUPER-TIGER Instrument: Measurement of Elemental Abundances of Ultra-Heavy Galactic Cosmic Rays. The Astrophysical Journal 788 (1), 18.

Bravar, U., Bruillard, P.J., Fluckiger, E.O., Macri, J.R., McConnell, M.L., Moser, M.R., Ryan, J.M., Woolf, R.S., 2006. Design and testing of a position-sensitive plastic scintillator detector for fast neutron imaging. Nuclear Science, IEEE Transactions on 53 (6), 3894–3903.

Cruceru, M., Cruceru, I., Litvinenko, A., Ciolacu, L., 2013. A Small-Area Scintillation Hodoscope Used for Components Test of MPD Detector in NICA Experiment. Universal Journal of Physics and Application 7 (4), 376–379.

Farías, R.O., Bortolussi, S., Menéndez, P.R., González, S.J., 2014. Exploring boron neutron capture therapy for non-small cell lung cancer. Phys. Med. 30 (8), 888–897.

Gerber, M.S., Miller, D.W., Schlosser, P.A., Steidley, J.W., Deutchman, A.H., 1977. Position sensitive gamma ray detectors using resistive charge division readout. Nucl. Sci. IEEE Trans. 24 (1), 182–187.

Ghal-Eh, N., Koohi-Fayegh, R., Hamidi, S., 2007. Low-energy neutron flux measurement using a resonance absorption filter surrounding a lithium glass scintillator. Radiat. Phys. Chem. 76 (6), 917–920.

Hatanaka, H., 1987. Neutron Capture Therapy.

McGregor, D.S., Lindsay, J.T., Olsen, R.W., 1996. Thermal neutron detection with cadmium 1 − x zinc x telluride semiconductor detectors. Nuclear Instruments and Methods in Physics Research Section A: Accelerators, Spectrometers, Detectors and Associated Equipment, vol. 381(2), pp. 498–501.

McKinney, G.W., Durkee, J., Hendricks, J., James, M., Johns, R., Pelowitz, D.B., Waters L. S., 2007. MCNPX 2.6. X features (2006-2007). Los Alamos National Laboratory Report LA-UR-07-2053, M&C/SNA.

Mostafaei, F., McNeill, F.E., Chettle, D.R., Matysiak, W., Bhatia, C., Prestwich, W.V., 2015. An investigation of the neutron flux in bone-fluorine phantoms comparing accelerator based in vivo neutron activation analysis and FLUKA simulation data. Nucl. Instrum. Methods Phys. Res. Sect. B: Beam Interact. Mater. Atoms 342, 249–257.

NIST website, ⟨http://physics.nist.gov/PhysRefData/XrayMassCoef/ElemTab/z82.html⟩.

Rassow, J., Stecher-Rasmussen, F., Voorbraak, W., Moss, R., Vroegindeweij, C., Hideghéty, K., Sauerwein, W., 2001. Comparison of quality assurance for performance and safety characteristics of the facility for boron neutron capture therapy in petten/NL with medical electron accelerators. Radiother. Oncol. 59 (1), 99–108.